Available online at www.eccomasproceedia.org
Eccomas Proceedia COMPDYN (2023) 5074-5088

ECCOMAS
Proceedia

COMPDYN 2023
9th ECCOMAS Thematic Conference on
Computational Methods in Structural Dynamics and Earthquake Engineering
M. Papadrakakis, M. Fragiadakis (eds.)
Athens, Greece, 12-14 June 2023

SEISMIC PERFORMANCE OF SPECIAL STEEL MOMENT FRAMES USING DETAILED VS SIMPLE HYSTERIC CURVES

E. Clavijo[1], J. Molina[1], N. Coello[1], X. Vintimilla[1], F. Flores [1] and P. Quinde[1]

[1] Department of Civil Engineering, University of Azuay
Cuenca 010204, Ecuador
{emiclavijoc, mpjorgel}@es.uazuay.edu.ec
{nicolas.coello99, xavier.vintimillas30}@ucuenca.edu.ec
{fflores, pabloquinde}@uazuay.edu.ec

Abstract

It is a common belief that modeling structures using bilinear materials with no strength or stiffness degradation perform better than modeling structures with more detailed materials that include degradation. This investigation focuses on the effects of modeling in two different ways the hysteretic curves of beams and columns in special steel moment resisting frames. The analyzed structure is an 8-Story Special Steel Moment Frame where its performance is measured by means of static and dynamic analyses. Inter-story drifts and energies are quantified at different intensity levels and using multiple ground motions to establish the difference of using a simple vs a detailed hysteretic curve. It was found that unlike what is commonly believed, structures modeled with a simple hysteretic behavior do not capture properly the seismic response of a structure. It was demonstrated that hysteretic energy dissipation is not an indicator of seismic performance.

Keywords: Energy Dissipation, OpenSees, Special Steel Moment Frames, FEMA P695.

ISSN:2623-3347
Peer-review under responsibility of the organizing committee of COMPDYN 2023.
doi: 10.7712/120123.10784.21141

1 INTRODUCTION

The study of the response of a structure subjected to earthquake-induced motion depends primarily on the quality of the mathematical model. Structures idealized with concentrated inelasticity elements can be modeled with a wide range of materials that represent their behavior under a cyclic load. It is commonly believed that the incorporation of a simple bilinear model will dissipate more energy due to the lack of strength degradation leading to a better seismic performance. As established by Kazantzi & Vamvatsikos [1] "It is no wonder then that higher energy dissipation seems to be equivalent to higher damping, ergo better performance". The purpose of this investigation is to evaluate the adequacy of using two different hysteretic curves with and without strength degradation in terms of energy dissipation, drift limits and collapse evaluation. This study tries to fill the void of previous investigations that focuses mainly on the effect of the hysteresis type on the global collapse drift limit [2]. Also, to verify the correlation between energy dissipation and the behavior of a structure subjected to different intensity level earthquakes.

Analyzing energy dissipation of a building during seismic loads helps to evaluate the ability of a structure to absorb and dissipate energy considering that each structural member contributes to energy dissipation. Damping energy is the energy that is diminished by different mechanisms as inherent and hysteretic when cycling forces or deformations occur. "Dynamic loading conditions differ as energy input and energy dissipation are intimately related with the details of the system's hysteresis" [1]. Hysteretic energy dissipation is often understood as a synonym of seismic performance as seen in many seismic codes. Recent studies question the truthfulness of this belief due to the limited evidence on it. Kazantzi & Vamvatsikos [3] demonstrated that energy dissipation is not an index of seismic performance. Therefore, there is an unconscious use the concept of energy dissipation.

The building used to perform the proposed analyses is found at NIST GCR 10-917-8 [4] report as the 4RSA 8-story Special Steel Moment Frame Archetype. The plastic hinges were defined in two different models, the first one using a simple bilinear hysteretic curve with strain hardening (Steel01) and the second one with a hysteretic curve that includes strength degradation (Bilin). Analyses were made to compare their performance using inter-story drifts and energy dissipation when multiple ground motions are applied. Far-Field ground motion record set (22 component pairs) provided by the FEMA P-695 [5] methodology was considered under different seismic intensities.

Furthermore, the collapse margin ratio (CMR) was computed according to the FEMA P-695 as the ratio of the median value of collapse level earthquake spectral acceleration, to the MCE spectral response acceleration at the fundamental period of the building. The median collapse intensity was obtained as the incremental dynamic factor for the structure to collapse with 22 out of 44 ground motions. According to Vamvatsikos & Cornell [6], a collapse occurs when the local tangent of an incremental dynamic analysis (IDA) curve reaches 20% of the elastic slope (first slope in the IDA curve), or when a story reaches a 10% drift, because it is unlikely that the structure will recover.

2 BUILDING OVERVIEW

2.1 Geometry

The building used for this investigation was taken from the NIST GCR 10-917-8 [4].The 8-story SMF designed with the modal response spectrum (RSA) was studied. The structure's design was followed according to the ASCE 7-05 [7]. The plan view layout of the structure is presented in Figure 1. The SMF consist of a 3-bay perimeter frame on each side with

prequalified reduced beam sections (RBS) connections. The bay width (centerline dimensions) is 6.1 m (20 ft). The height of the first story is 4.6 m (15 ft) and the height of all other stories is 4 m (13 ft). The member sizes were assigned according to the NIST [4] archetype data. Axial reduction of the columns was contemplated as required by the FEMA P-695 [5] methodology.

2.2 Design Loads

According to the NIST [4] the dead load (*D*) was 4.31 kN/m^2 (90 psf) uniformly distributed over each floor and a cladding load was applied as a perimeter load of 1.2 kN/m^2 (25 psf). The design life load (*L*) was 2.4 kN/m^2 (50 psf) on all floors and 0.96 kN/m^2 (20 psf) on the roof. Loads were distributed on the tributary areas as shown in Figure 1.

The recommended load combination considered to obtain the acting loads and the corresponding story masses is 1.05*D*+0.25*L*.

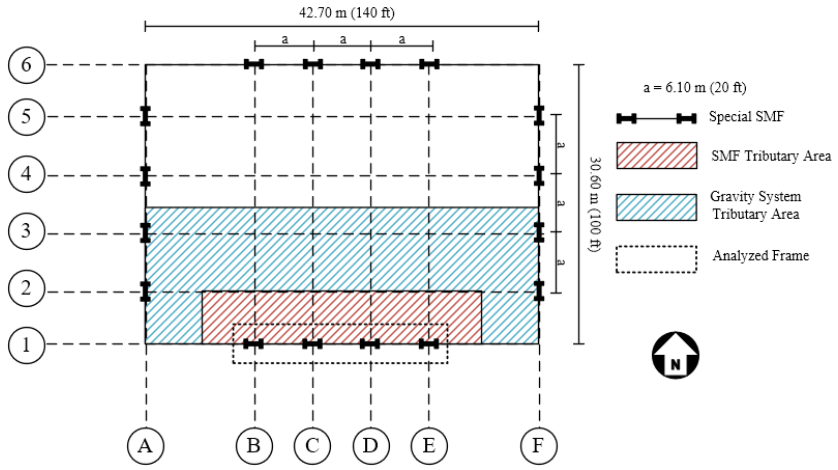

Figure 1: Building plan view layout.

3 NONLINEAR MODEL

3.1 Hysteresis Type

The models and analyses were carried out via OpenseesPy [8] as it allows the utilization of an extended number of materials that can be studied for the objective of this investigation. The selected materials as presented in Figure 2 were Steel01 as the simple material and the Modified Ibarra-Medina-Krawinkler Deterioration Model with Bilinear Hysteretic Response (Bilin Material) as the detailed one. Beams and columns were incorporated by using elastic elements with plastic hinges (zero-length elements) at the ends of the elements. The hysteretic behavior of beams and columns considers one model with stiffness and strength degradation and other with a simplified model with no deterioration.

The modeling of the Bilin and Steel01 materials were made according to Dimitrios Lignos' investigation [9]. The calibration parameters of plastic hinges were considered according to the w-section properties.

Hysteretic curves presented below were obtained to verify the correct behavior of the materials incorporated in the models. Figure 2 corresponds to a plastic hinge of the 1st story beam W30x108.

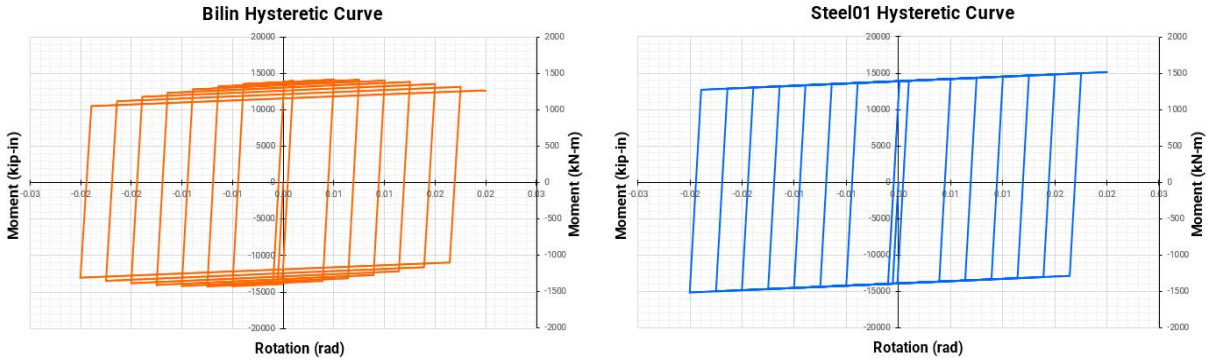

Figure 2: Beam W30x108 hysteretic behavior.

Panel zones were modeled using a rectangular region composed with eight rigid elements and a nonlinear rotational spring on the right top corner defined by a hysteretic material [10]. Connections at the base of the columns are fixed and compounded by very stiff plastic hinges.

3.2 P-Delta considerations

Geometric nonlinearities were incorporated using a leaning column with no flexural stiffness to consider P-Delta effects of the seismic mass that is not tributary to the frame (one-half the load of the gravity system) [5]. It consists of elements with end-to-end releases that are joined to the structure by truss-like elements. Moment transmission is not permitted and the stiffness of the seismic-force-resisting system is not compromised. The resulting model is shown in Figure 3, which provides a visual representation of the structure used in the analyses.

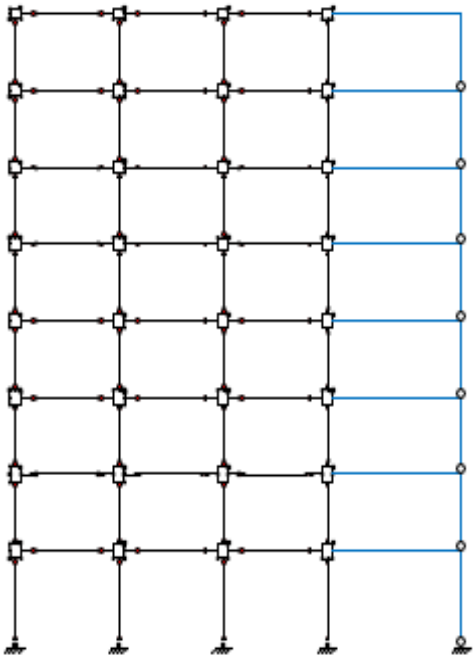

Figure 3: Mathematical model of the 4RSA 8-story building.

4 GROUND MOTIONS SCALING METHOD

As mentioned previously, the 22 horizontal component pairs of Far-Field records with similar characteristics provided by the FEMA P-695 [5] were used to perform the analyses in this investigation. Scaling process as shown in Figure 4 was necessary to perform nonlinear dynamic analysis.

The FEMA P-695 was also followed to scale the ground motions. This two-step process involves first normalizing the individual ground motions by their respective PGVs, and second, scaling the records to the MCE intensity at the fundamental period of the analyzed archetype.

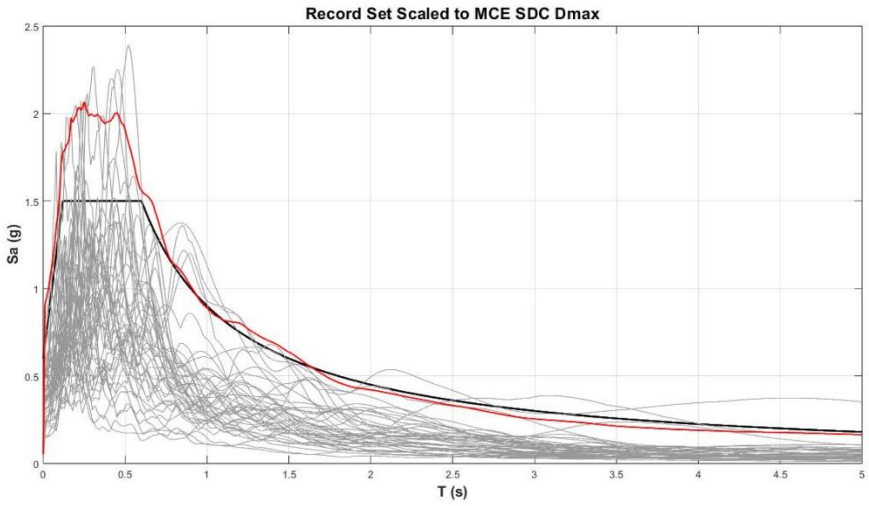

Figure 4: Median spectrum of the Far-Field record set anchored to the MCE.

5 MODEL BEHAVIOR CHECKS

It is required to make some model behavior checks to verify that the characteristics of the modeled building matches the archetype data proposed by the NIST report. These procedures assure somehow the reliability of the mathematical model when evaluating seismic performance and the results to be precise. It is important to conduct linear checks such as Modal Analysis, Free Vibration and to perform nonlinear analysis such as Pushover Analysis and its Sequence of Yielding.

5.1 Modal Analysis

Firstly, the modes and mass participation factors of the structure were analyzed in order to compare with the ones reported by the NIST. The corresponding value of the natural frequency of the selected system is $T=2.29s$ as shown in Table 6-4 of the NIST [4]. Accordingly, the results obtained in both Steel01 and Bilin models were computed as 2.28s as shown in Figure 5 that displays the concordance with the archetype.

All the modes obtained by the modal analysis and their respective participation mass factors are summarized in Table 1.

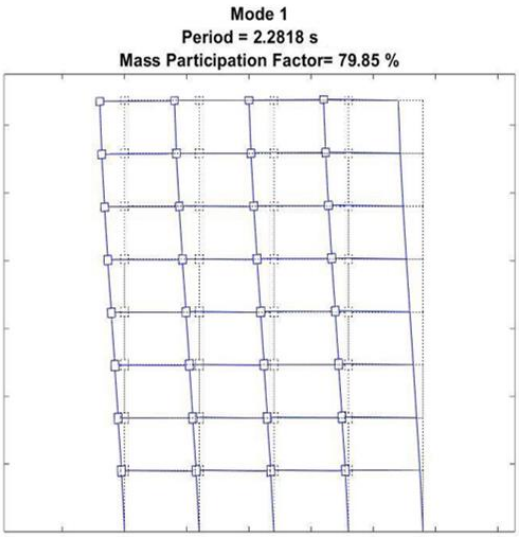

Figure 5: Fundamental Mode of Vibration of the systems.

Mode	Period (s)	MPF (%)
1	2.2818	79.85
2	0.7936	12.75
3	0.4349	3.8
4	0.2791	1.83
5	0.1981	0.98
6	0.1467	0.47
7	0.1141	0.23
8	0.0919	0.09

Table 1: Summary of Modal Analysis.

5.2 Free Vibration

As the rate at which the motion decays is controlled by the damping ratio, it is correct to use a free vibration analysis to prevent wrong damping assumptions. In this way, the actual damping presented by the model is ensured to avoid high damping forces that are hard to identify in areas of concentrated inelasticity, which can lead to an invalid analysis [11]. The obtained damping ratio was 2.43% compared to the Rayleigh's damping ratio of 2.5% assigned to the first and third modes, as shown in Figure 6.

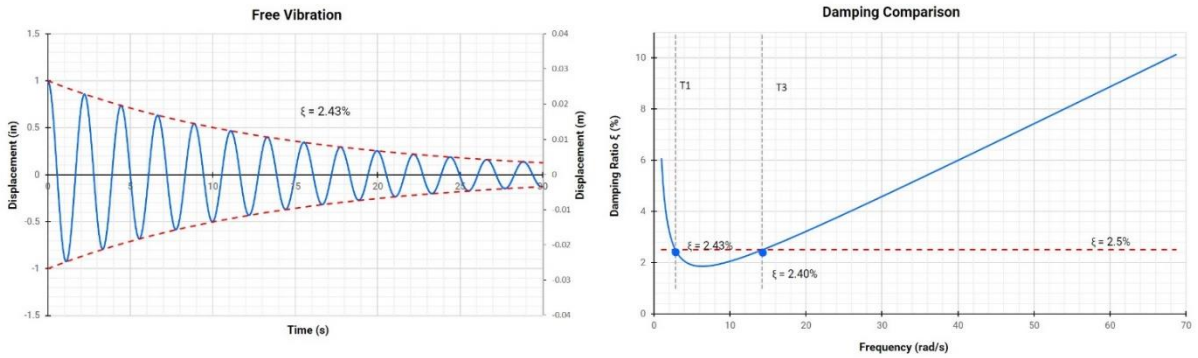

Figure 6: Rayleigh's damping obtained by logarithmic decay of Free vibration.

It is important to check the assumed damping assigned to each mode. It is very easy to lose the sense of the effective damping that the mathematical model has if this step is omitted. Table 2 shows the computed Rayleigh's damping value of each mode compared to the one assigned by OpenSees.

Mode	Real Damping (%)	Theoretical Damping (%)
1	2.43	2.5
2	1.87	1.91
3	2.4	2.5
4	3.48	3.59
5	4.84	4.86
6	6.32	6.44
7	7.98	8.2
8	10.05	10.13

Table 2: Real damping of the structure and Rayleigh's theoretical damping.

5.3 Pushover checks

Pushover analysis was performed to evaluate different parameters such as overstrength, ductility and secondary stiffness. According to Table 6-9 of the NIST [4], the archetype was presented with an overstrength of Ω=3.27 and a ductility value of μ=2.74. Figure 7 shows that both models have near values of overstrength and ductility that can be accepted to represent the NIST model. Ductility and post yield negative stiffness depend on the complexity of the hysteretic model.

The procedures presented in this section help to both validate the model and verify the values presented by the NIST report, also provide insight of the hysteretic behavior effects. These checks are important to ensure that the upcoming analyses present the correct results.

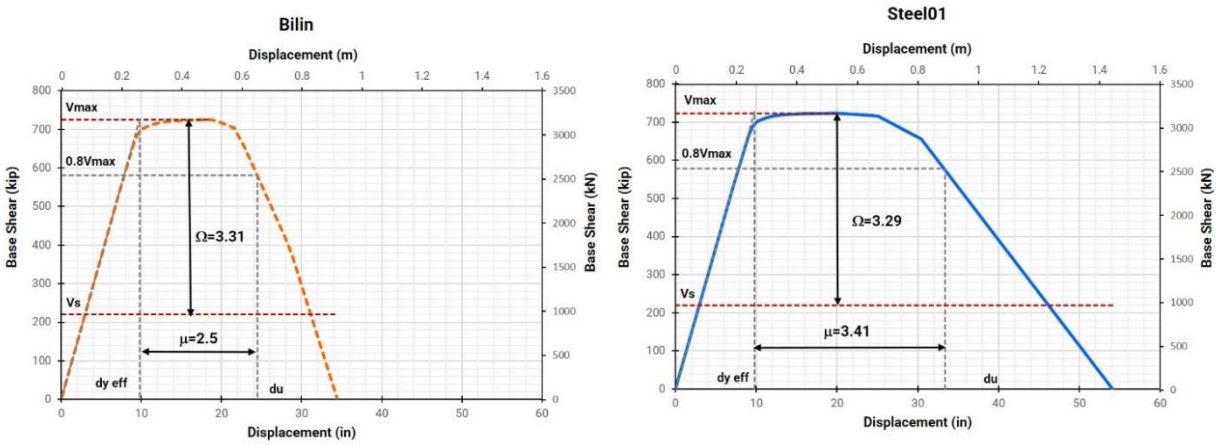

Figure 7: Pushover results of ductility and overstrength of the models.

Nonlinear incremental static analysis was performed by assigning a lateral load according to the shape of the first vibration mode to obtain the capacity curve of the models. Plastic hinges develop stiffness changes that can be visualized on the sequence of yielding of the structure. As shown in Figure 8 the mathematical model displays a correct damage behavior in both models. The plastic hinges at the bases of the structure yield first, followed by the beams and finally the columns of the 1st and 2nd stories.

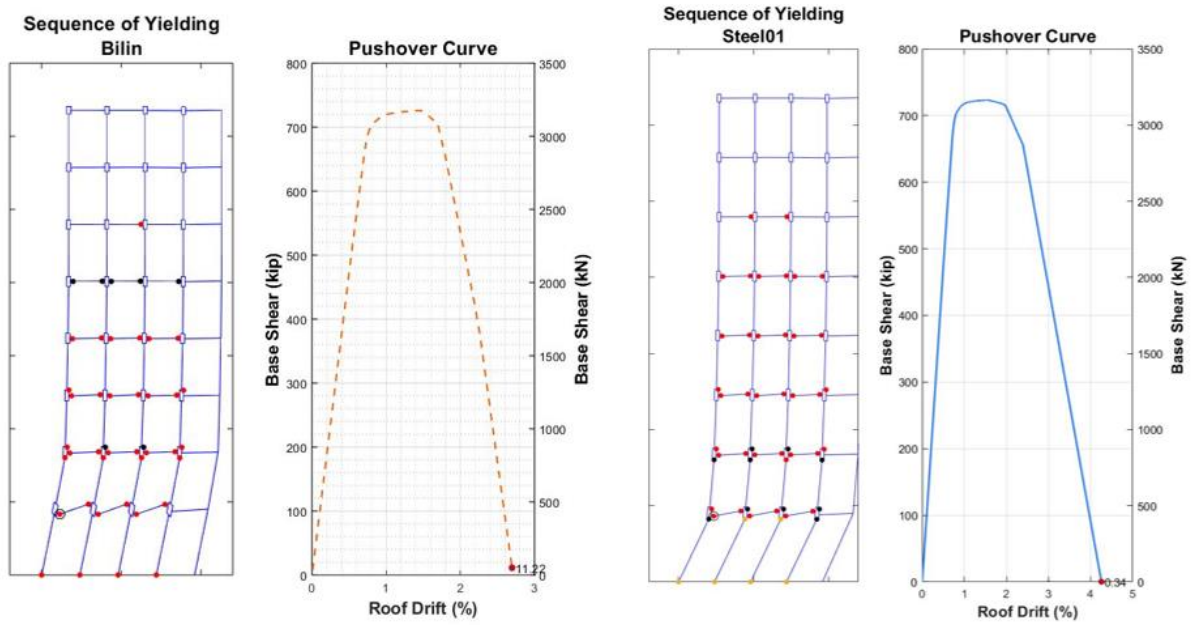

Figure 8: Sequence of yielding of the models.

6 RESULTS

Based on the work presented herein, results of a comparison between the simple and detailed models are provided. The analyses performed include nonlinear time history (NTH) analysis, energy dissipation, and collapse margin evaluation.

The comparison of the results provides a comprehensive view of the seismic behavior and performance of both models.

6.1 Nonlinear Static Pushover Analysis

In this approach, base shear vs roof displacement curves were considered with and without P-Delta effects. It can be seen that P-Delta effects are significant for buildings with a considerable number of stories as shown in Figure 9. Negative stiffness occurs due to two main reasons: material degradation and P-Delta effects. For these structures, P-Delta effects might be the factor that contributes the most to the seismic performance of the structure, thus causing the amplification of story drifts. When the roof drift reaches 1.35%, the corresponding 1st story drift is 2.29%. At this point it can be seen that both models start to show differences and the Steel01 model largely surpasses the Bilin's capacity. The capacity of the Bilin material is compromised due to the material degradation that can be seen on the secondary stiffness of its pushover curve.

Inter-story drifts in lower stories must be checked since SSMFs tend to concentrate story drifts in lower levels [12].

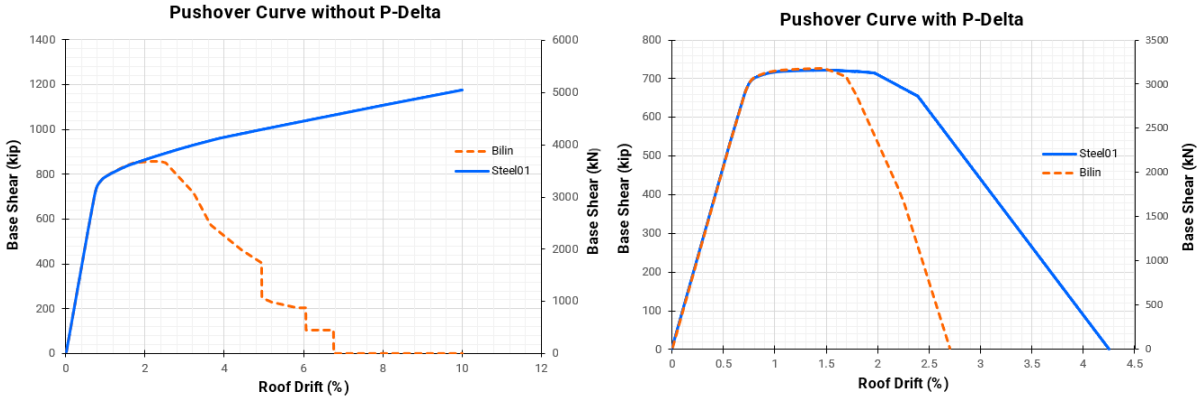

Figure 9: Pushover curves with and without P-Delta effects.

6.2 Nonlinear Time History Analysis

NTH analyses were performed following the FEMA P-695 methodology [5]. Two intensities such as the MCE and higher intensities determined by IDAs were selected. The analyses were conducted with and without P-Delta effects to compare their influence on the seismic behavior of an 8-story SMF building. Second-order effects are essential on predicting the earthquake response of buildings that have significant deformations into their inelastic range [13].

Figure 10 shows the first-story drifts at the MCE intensity, including P-Delta effects for two different ground motions. It can be observed that the MCE intensity is not high enough to show a difference between the models' drifts. This occurs because there is not enough damage induced at the hinges, as follows both hysteretic curves will have the same results. The analyses were computed for every Far-Field ground motion record, but only two were selected to be presented.

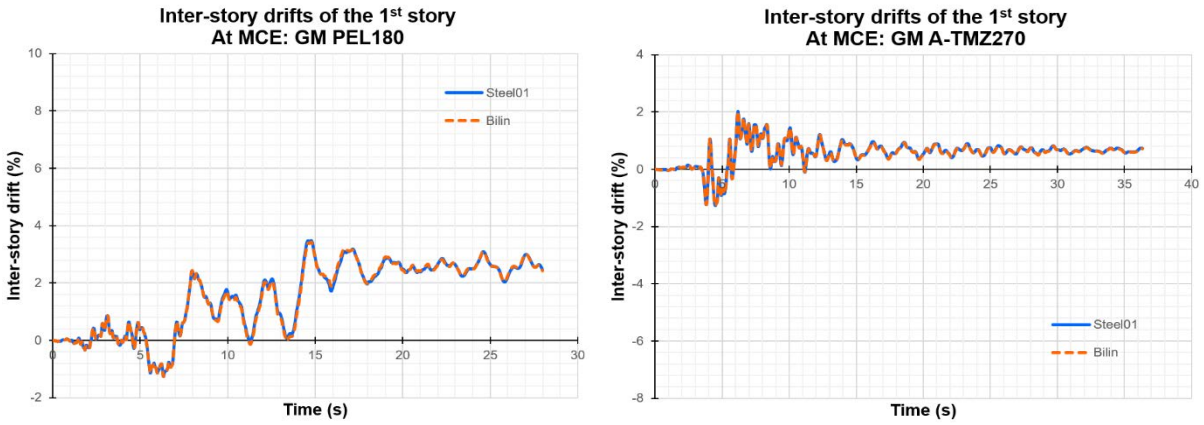

Figure 10: First story drifts at the MCE intensity with P-Delta effects.

The same ground motions, at higher intensities are shown in Figure 11. The Bilin model clearly shows larger drifts, which means it will collapse before than the Steel01. In addition to the significant influence of P-Delta effects at higher intensities, it is important to consider the strength degradation of the material. As stated by Ibarra et al. [14], "results from the seismic evaluation of various systems demonstrate that strength deterioration becomes a dominant factor when the response of a structure approaches the limit state of collapse". The Bilin behavior presented below shows the influence of both factors. On the contrary, Steel01 is not conditioned by the deterioration phase, this is the reason why P-Delta effects are better received

by this material. It can be clearly seen that Steel01 does not capture large displacements in the same way that the Bilin model does.

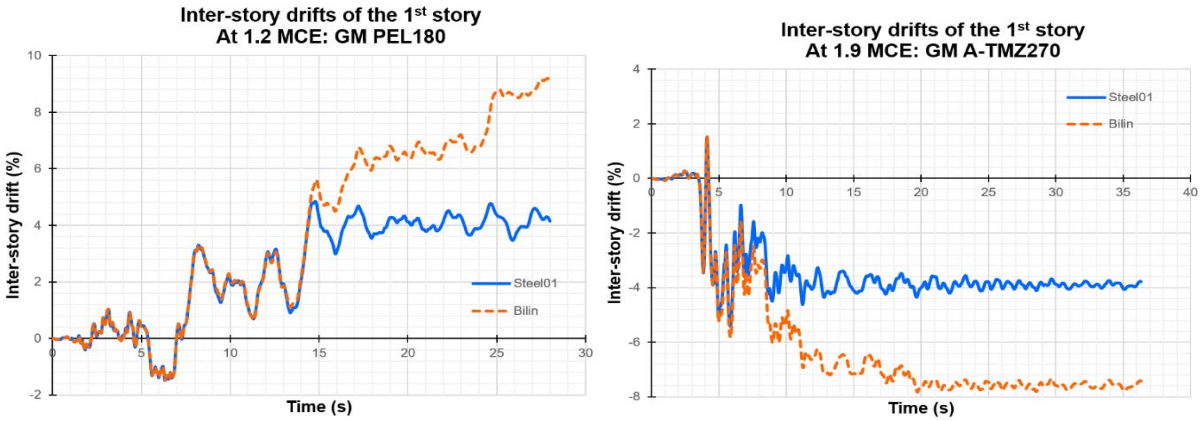

Figure 11: First story drifts at higher intensities with P-Delta effects.

When P-Delta effects are not considered, both models show similar first-story drifts throughout the entire motion as shown in Figure 12. It can be seen that grey lines represent P-Delta effects that are considerably increasing inter-story drifts compared to the results without P-Delta. These results demonstrate that P-Delta effects are more significant than strength degradation in this building model.

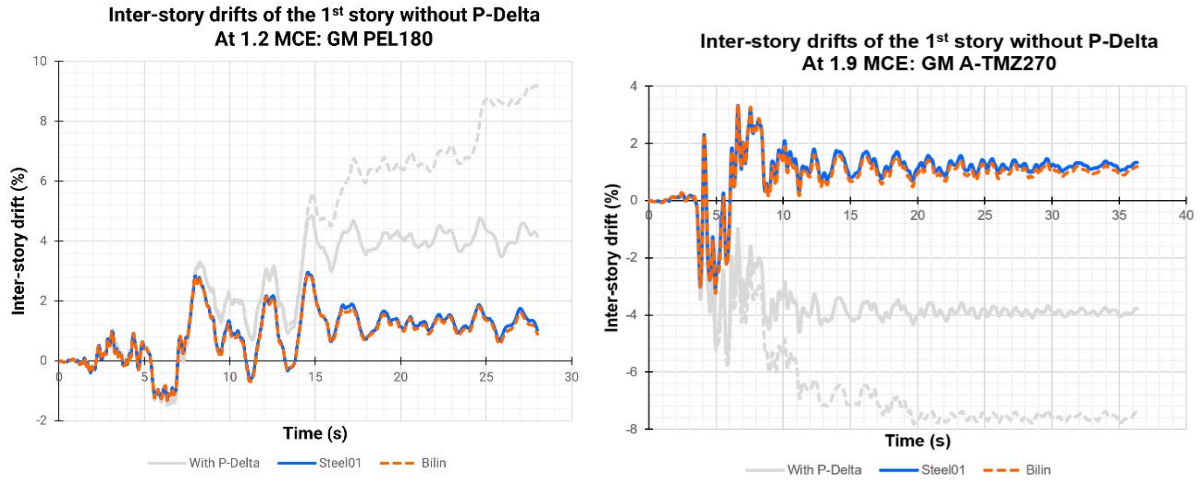

Figure 12: First story drifts at higher intensities without P-Delta effects.

6.3 Energy Dissipation

Input, kinetic, inherent damping, hysteretic damping, potential and total energy were considered to obtain the energy balance of the structure considering P-Delta effects.

At the MCE intensity, both models have approximately the same energy dissipation as shown in Figure 13 for two different ground motions. Therefore, their displacements are almost the same (Figure 10). The Bilin material has not been subjected to enough stress to develop the strength degradation phase so it behaves similarly to Steel01.

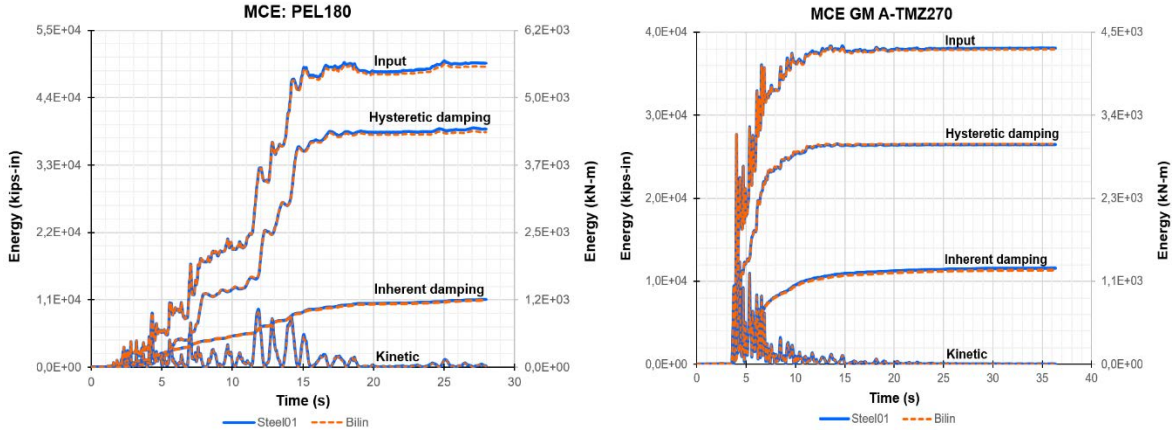

Figure 13: Energy balance at the MCE intensity.

At higher intensities, hysteretic energy has the largest differences because it is related to the moment-rotation curve which depends directly on the material behavior.

There are two possible cases that can occur, considering that the detailed model always develops the largest drifts as shown in Figure 11. First, the Steel01 model dissipates more energy as shown in Figure 14. It can be noticed that the Steel01 model has a higher hysteretic energy and a better behavior in this case.

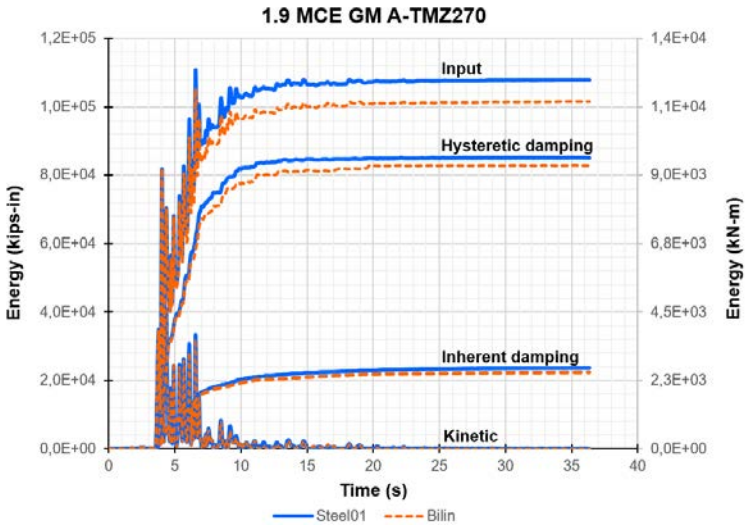

Figure 14: Energy balance of A-TMZ270 at higher intensities.

Second, contrary to what is believed there are several cases where the Bilin model dissipates more energy as shown in Figure 15 and has a worse performance as it reaches higher drifts.

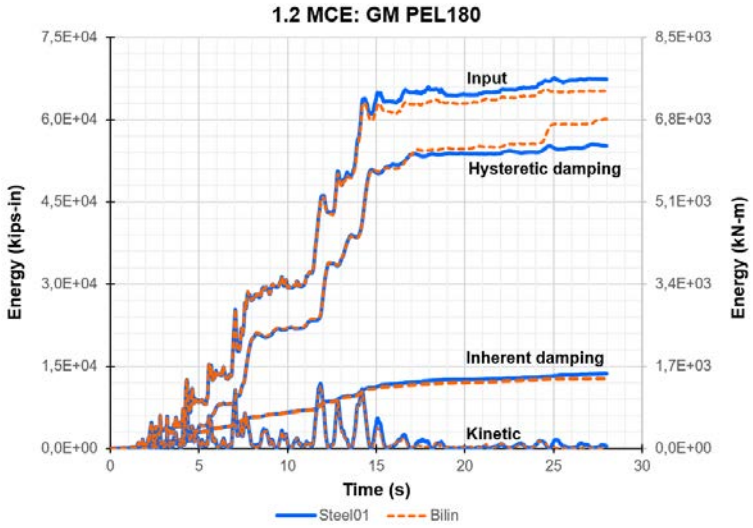

Figure 15: Energy balance of PEL180 at higher intensities.

As found in the analyses, it is not possible to determine which model has a better seismic performance by analyzing energies only. These results do not provide the accurate information about the damage that this structure can develop. Although in some cases the Steel01 model can reach higher energy dissipation, the Bilin model for this study always had larger drifts. These energies results cannot determine the seismic performance evaluation of the structure.

6.4 Collapse Evaluation

Using the OpenSees software, IDAs considering P-Delta effects were conducted until any inter-story drift reached 10%. In order to calculate the median with two-decimal precision, the stepping method proposed by Hardyniec & Charney [15] was applied. The summary of the computed results is shown in Figure 16 as IDA curves. A flattening can be seen at the end of the curves, indicating that a collapse was reached.

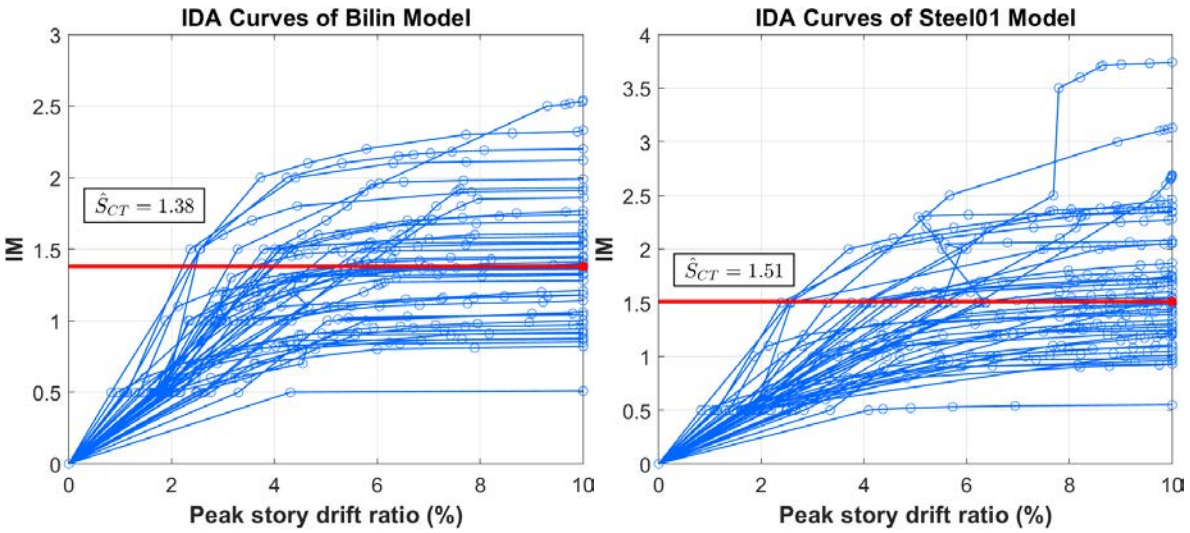

Figure 16: Incremental Dynamic Analyses Curves of the models.

There is a specific factor for each ground motion that causes the structure to collapse, these factors were plotted against the probability of collapse. The fragility curve was fitted following the explanation of Porter et al. [16], which estimates the logarithmic standard deviation through

an equation. In addition, the previously obtained median collapse intensity was used in the fitting. Figure 17 presents the fragility curves with the corresponding CMR of both models. It can be seen that Bilin has a lower CMR and it closely matches the value reported by NIST of a *CMR=1.42*, as shown in Table 3.

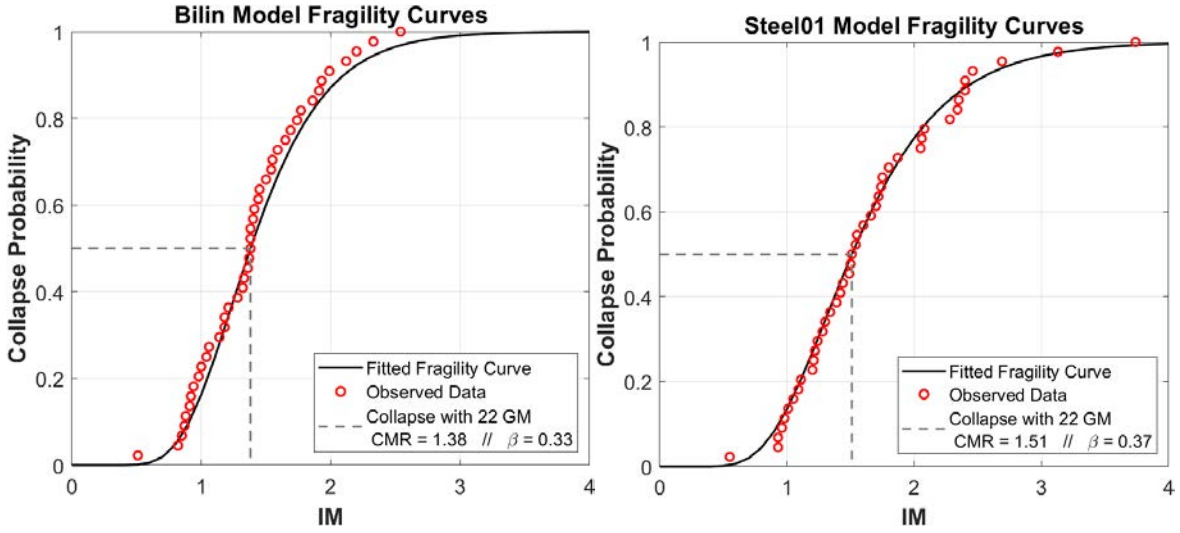

Figure 17: Fragility curve and CMR computation of the models.

Model	CMR
NIST	1.42
Steel01	1.51
Bilin	1.38

Table 3: CMR comparison of the NIST and the models analized.

7 CONCLUSIONS

In this paper, it was presented a seismic performance evaluation when modeling an 8-story SMRF with the Bilin material that represents a hysteretic model with strength degradation and the Steel01 material that represents a simple bilinear model with no degradation.

The purpose of the study was to determine the level of detail that the hysteretic model should have to obtain the most accurate mathematical model. The effect of the hysteresis type based on the results described previously lead to the following conclusions:

1) Energy dissipation cannot provide enough information to determine which material will have a better seismic performance on a structure. The simplified model that has no strength degradation (Steel01) does not properly capture large displacements that the structure can reach. There are parameters such as ductility, secondary stiffness or the post yield slope that are better indicators of seismic performance.
2) According to the NTH analyses results, it can be concluded that the material with strength degradation (Bilin) is always the first one collapsing. Therefore, strength and stiffness degradation are necessary to capture large displacements.
3) The post yield capacity of a structure is mainly conditioned by two parameters: secondary order effects and material degradation. In this study P-Delta effects controlled over degradation due to the height of the structure. Further investigation needs to be done in shorter buildings to explore the influence of strength degradation and P-Delta effects.

4) Inherent damping energy of approximately 20% of the input energy was reached by incorporating a damping ratio of 2.5%. Additional investigation can be done to analyze the influence of higher damping ratio on the contribution of inherent damping in the energy dissipation and the structure's collapse evaluation.
5) Hysteresis type becomes significant when the structure approaches to a collapse state. The structural response is impacted by the level of detail of the hysteretic and capacity curves in ways that cannot be described by energy dissipation. The simple hysteretic behavior can be incorporated when drifts are limited to short displacements.

8 ACKNOWLEDGEMENTS

The work presented herein was possible through the financial support of the University of Azuay in Cuenca-Ecuador.

REFERENCES

[1] A. K. Kazantzi and D. Vamvatsikos, "A study on the correlation between dissipated hysteretic energy and seismic performance," 2012.
[2] Z. Huang and D. A. Foutch, "Effect of hysteresis type on drift limit for global collapse of moment frame structures under seismic loads," *Journal of Earthquake Engineering*, vol. 13, no. 7, pp. 939–964, Sep. 2009, doi: 10.1080/13632460902859144.
[3] A. K. Kazantzi and D. Vamvatsikos, "The hysteretic energy as a performance measure in analytical studies," *Earthquake Spectra*, vol. 34, no. 2, pp. 719–739, May 2018, doi: 10.1193/112816EQS207M.
[4] NIST, "Evaluation of the FEMA P-695 Methodology for Quantification of Building Seismic Performance Factors NEHRP Consultants Joint Venture A partnership of the Applied Technology Council and the Consortium of Universities for Research in Earthquake Engineering," 2010.
[5] Fema, *Quantification of Building Seismic Performance Factors*. 2009. [Online]. Available: www.ATCouncil.org
[6] D. Vamvatsikos and C. A. Cornell, "Applied incremental dynamic analysis," *Earthquake Spectra*, vol. 20, no. 2, pp. 523–553, 2004, doi: 10.1193/1.1737737.
[7] ASCE, "SEISMIC DESIGN REQUIREMENTS FOR BUILDING STRUCTURES 12.1 STRUCTURAL DESIGN BASIS 12.1.1 Basic Requirements," 2005.
[8] F. McKenna and F. Gregorie, "OpenSees." 2000.
[9] D. Lignos and H. Krawinkler, "SIDESWAY COLLAPSE OF DETERIORATING STRUCTURAL SYSTEMS UNDER SEISMIC EXCITATIONS," 2012. [Online]. Available: http://blume.stanford.edu
[10] A. Gupta and H. Krawinkler, "SEISMIC DEMANDS FOR PERFORMANCE EVALUATION OF STEEL MOMENT RESISTING FRAME STRUCTURES," 1999. [Online]. Available: http://blume.stanford.edu
[11] F. A. Charney and F. Asce, "Unintended Consequences of Modeling Damping in Structures," pp. 1–12, 2008, doi: 10.1061/ASCE0733-94452008134:4581.
[12] F. X. Flores, B. X. Astudillo, and S. Pozo, "Effective Modeling of Special Steel Moment Frames for the Evaluation of Seismically Induced Floor Accelerations," *Journal of Structural Engineering*, vol. 147, no. 1, Jan. 2021, doi: 10.1061/(asce)st.1943-541x.0002851.

[13] A. K. Chopra, "DYNAMICS OF STRUCTURES Theory and Applications to Earthquake Engineering Fifth Edition in SI Units," 2020.
[14] L. F. Ibarra, R. A. Medina, and H. Krawinkler, "Hysteretic models that incorporate strength and stiffness deterioration," *Earthq Eng Struct Dyn*, vol. 34, no. 12, pp. 1489–1511, 2005, doi: 10.1002/eqe.495.
[15] A. Hardyniec and F. Charney, "A new efficient method for determining the collapse margin ratio using parallel computing," *Comput Struct*, vol. 148, pp. 14–25, 2015, doi: 10.1016/j.compstruc.2014.11.003.
[16] K. Porter, R. Kennedy, and R. Bachman, "Creating fragility functions for performance-based earthquake engineering," *Earthquake Spectra*, vol. 23, no. 2, pp. 471–489, 2007, doi: 10.1193/1.2720892.